

2QAN: A quantum compiler for 2-local qubit Hamiltonian simulation algorithms

Lingling Lao, Dan Browne

Department of Physics and Astronomy, University College London, London WC1E 6BT, United Kingdom

Abstract

Simulating quantum systems is one of the most important potential applications of quantum computers to demonstrate its advantages over classical algorithms. The high-level circuit defining the simulation needs to be transformed into one that compiles with hardware limitations such as qubit connectivity and hardware gate set. Many techniques have been developed to efficiently compile quantum circuits while minimizing compilation overhead. However, general-purpose quantum compilers work at the gate level and have little knowledge of the mathematical properties of quantum applications, missing further optimization opportunities. In this work, we exploit one application-level property in Hamiltonian simulation, which is, the flexibility of permuting different operators in the Hamiltonian (no matter whether they commute). Conventional compilation techniques may not be directly adapted to this flexibility because changing the order of anti-commuting gates violates program semantics.

We develop a compiler, named 2QAN, to optimize quantum circuits for 2-local qubit Hamiltonian simulation problems, a framework which includes the important quantum approximate optimization algorithm (QAOA). In particular, we propose permutation-aware qubit mapping, qubit routing, gate optimization and scheduling techniques to minimize the compilation overhead. We evaluate 2QAN by compiling three applications (up to 50 qubits) onto three quantum computers that have different qubit topologies and hardware two-qubit gates, namely, Google Sycamore, IBMQ Montreal and Rigetti Aspen. Compared to state-of-the-art quantum compilers, 2QAN can reduce the number of inserted SWAP gates by up to 11.5X, reduce overhead in hardware gate count by up to 30.7X, and reduce overhead in circuit depth by up to 21X. This significant overhead reduction will help improve application performance. Experimental results on the Montreal device demonstrate that benchmarks compiled by 2QAN achieve highest fidelity.

1. Introduction

Quantum simulation has broad applications in quantum many-body physics [1], quantum chemistry [2], and quantum field theory [3] and has been demonstrated in different quantum technologies [4, 5] (see [6] for a detailed review). The problem of Hamiltonian simulation can grow exponentially with respect to the system size, becoming intractable by classical computers for large systems. Quantum computers can be used

to efficiently solve this problem, as first proposed by Richard Feynman [7]. The main challenge is to find an efficient circuit that asymptotically approximates the time evolution of a Hamiltonian. Different approaches have been proposed for efficient Hamiltonian simulation, including product formulas [8, 9], Taylor series [10], quantum walk [11], and quantum signal processing [12]. The product formula has a straightforward implementation and good performance in practice [13, 14]. Given a Hamiltonian that is decomposed as a sum of Hermitian terms ($H = \sum_{j=1}^L h_j H_j$), the product formula approximates the exponent of this Hamiltonian as a product of exponents of individual terms and each individual exponent can be efficiently implemented by a quantum circuit. The approximation errors are caused by the anti-commuting terms in the Hamiltonian. To achieve a desired precision, the product is divided into many repetitions of small time steps, the circuit therefore has a periodic structure.

This high-level circuit representation is typically hardware-agnostic and needs to be decomposed into the gate set supported by the underlying quantum hardware. In noisy intermediate-scale quantum (NISQ) computers [15], the universal gate set is normally composed of arbitrary single-qubit rotations and one or a few two-qubit gates (e.g., the SYC, CNOT, iSWAP gates in quantum processors from Google, IBM, Rigetti respectively in Figure 1). Furthermore, these quantum computers only allow two-qubit gates on restricted qubit pairs, i.e., limited qubit connectivity. Compilation techniques are required to map circuit qubits onto hardware qubits and insert SWAP gates to move qubits to be neighbours, increasing circuit size in terms of gate count and circuit depth. In addition, two-qubit gates have much higher error rates than single-qubit rotations and qubits have short coherence time [16]. Therefore, it is critical to minimize compilation overhead for high-fidelity circuit implementation.

Many approaches have been proposed for compiling quantum circuits onto NISQ computers [19, 20, 21, 22, 23, 24]. These compilers operate at the gate level and are designed for general circuits with little knowledge regarding the mathematical properties of target applications. Exploiting the synergy between applications and compilation techniques can provide more optimizations on the implementation circuit, which will further improve application performance. For the quantum simulation problems, one application-specific property is the flexible ordering of different terms in the Hamiltonian. That

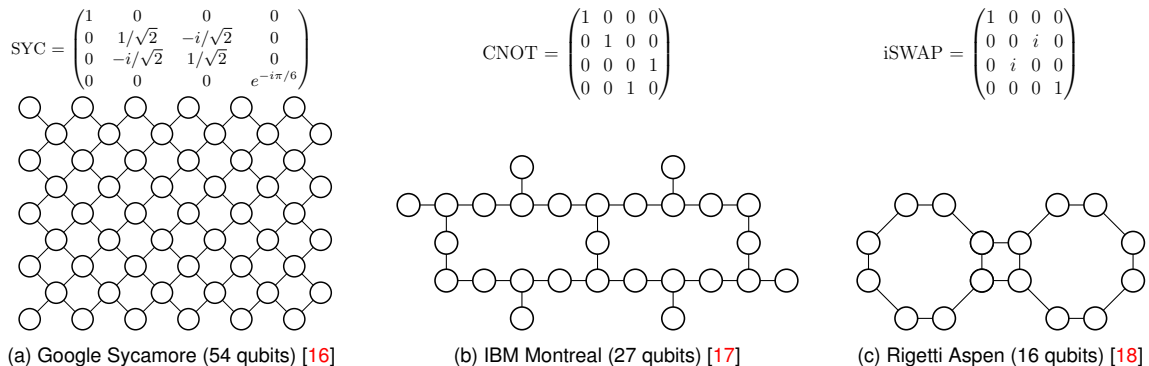


Figure 1: Device topologies and hardware two-qubit gates of different quantum computers. Nodes represent qubits and edges represent the connectivity between qubit pairs.

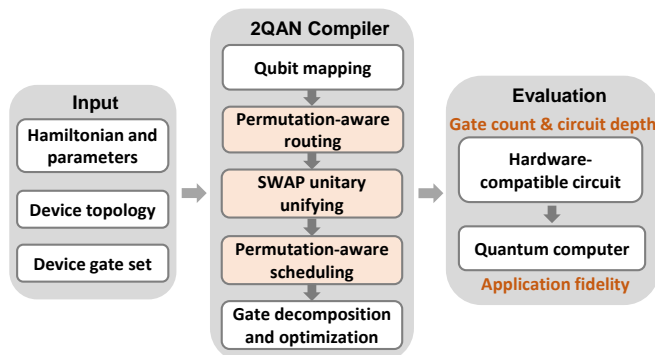


Figure 2: Overview of the 2QAN compiler. The highlighted compilation passes exploit the application-level semantics and cannot be replaced by general-purpose compilation techniques. Other passes are implemented by existing tools.

is, one could permute the exponents of these terms without losing computational accuracy. This is, however, difficult or even impossible to be recognized at the gate level, especially when many of these operators anti-commute with each other.

In this work, we identify this flexibility in Hamiltonian operator permutation and exploit it in the circuit compilation procedure. In particular, we propose novel qubit routing, gate scheduling, and gate optimization techniques to efficiently compile circuits for 2-local qubit Hamiltonian simulation problems. The quantum approximate optimization algorithm (QAOA) [25] also has Hamiltonians in this form. The developed compiler, named **2QAN**¹, can target different qubit topologies and different gate sets. Evaluation results on three quantum computers show that 2QAN can significantly reduce gate count and circuit depth compared to state-of-the-art quantum compilers. Furthermore, we also experimentally demonstrate the advantages of 2QAN on the IBMQ Montreal device. The evaluation toolflow is presented in Figure 2.

The main contributions of this work are:

¹Pronounced "toucan". We propose the name 2QAN since this compiler targets 2-local Qubit Hamiltonian simulation, is hardware Adapted and designed for Nisq quantum devices.

- We discover an optimization opportunity for compiling quantum simulation problems on NISQ computers, that is, the order of different terms in a Hamiltonian is flexible and a quantum compiler can permute their exponents (operators in the product formula) to minimize compilation overhead.
- We exploit this flexibility and develop 2QAN, a quantum compiler for efficiently compiling 2-local qubit Hamiltonian simulation problems on NISQ computers. We first propose a permutation-aware qubit routing heuristic to minimize the number of inserted SWAP gates. Then we implement a unitary unifying pass that combines a SWAP gate with a circuit gate to further reduce gate overhead. Moreover, we design a permutation-aware gate scheduling technique to minimize circuit depth. Both the routing and scheduling algorithms have linear time complexity in the number of gates and is therefore scalable for large systems.
- We evaluate the proposed compiler by compiling the Heisenberg model, the Ising model, and the QAOA circuits onto three industrial quantum computers, Google Sycamore [16], IBMQ Montreal [17], Rigetti Aspen [18]. We compare our 2QAN compiler with two state-of-the-art industrial compilers, t|ket) [26] and Qiskit [27]. Across all benchmarks and quantum computers, 2QAN can reduce the SWAP count by up to 6.7x (11.5x), the two-qubit gate overhead by up to 19x (30.7x), and depth overhead by up to 9.5x (21x) compared to t|ket) (Qiskit). Furthermore, experimental results of running QAOA on the IBMQ Montreal device show that this substantial compilation overhead reduction provides significant improvement in application performance. 2QAN achieves the highest fidelity for all problem sizes and can increase the QAOA layers while the other compilers cannot.

2. Background

2.1. Quantum simulation

Consider a system Hamiltonian H that is decomposed into a sum of polynomially many Hermitian terms H_j , $H = \sum_{j=1}^L h_j H_j$, its time evolution can be described by the unitary $U = \exp(it \sum_{j=1}^L h_j H_j)$. The goal is to find an efficient circuit

construction for this unitary. One of the leading approaches is the product formula or the Trotter formula [8, 9, 28],

$$V(t) = \prod_{j=1}^L \exp(it h_j H_j) \quad (1)$$

and each individual operator $V_j(t) = \exp(it h_j H_j)$ can be efficiently implemented by a quantum circuit. $V(t) = U$ if all the terms commute (i.e., $H_j H_k = H_k H_j$). $(V(t/r))^r$ approximates U for large r if some terms do not commute (which is typically the case in natural physical systems). This algorithm is referred as the first-order approximation. $V(t/r)$ is called one *Trotterization step* and the circuit has r such repetitions.

Operator permutation: Note that the order of terms in the Hamiltonian can be chosen from any of the $L!$ permutations. This flexibility allows one to optimize the Hamiltonian simulation circuit by *rearranging the individual operators* ($V_j(t)$) in the product formula (Equation 1). Such rearrangement is not trivial for general-purpose quantum compilers. This is because some of the operators anti-commute and reordering them at the gate level will cause logic violations in the compilation. Nevertheless, optimizing each Trotter step will improve the overall circuit construction since a large number of repetitions (r) need to be performed to achieve an error threshold ϵ , which will be the focus of this work. Moreover, reducing r will give further savings on the simulation cost. Many algorithms have been proposed, including higher-order approximations and randomization. For example, the second-order approximation

$$V_2(t) = \prod_{j=1}^L \exp(it h_j H_j / 2) \prod_{j=L}^1 \exp(it h_j H_j / 2) \quad (2)$$

can reduce r from $O((tL\Lambda)^2/\epsilon)$ (first-order) to $O((tL\Lambda)^{1+\frac{1}{2}}/\epsilon^{\frac{1}{2}})$ [28], Λ is the magnitude of the strongest term. Childs et al [29] and Campbell [30] show that randomizing how the operators are ordered can provide more improvements than a fixed permutation in each Trotter step.

2-local qubit Hamiltonian: In this work we consider 2-local qubit Hamiltonians that originate in many physical systems

$$H = \sum_{(u,v) \in E} H_{uv} + \sum_{k \in V} H_k, \quad (3)$$

where H_{uv} are two-qubit Hamiltonian terms and H_k are single-qubit Hamiltonians. The interaction graph of this Hamiltonian is represented by $G(V, E)$, V is the set of qubits and E is the set of edges. The Ising model, Heisenberg model, and XY model all have Hamiltonians in this form.

2.2. Circuit compilation

NISQ computers have hardware limitations such as native gate set and qubit connectivity, making quantum applications not directly executable. A hardware gate set is typically composed of arbitrary single-qubit rotations and a few two-qubit gates which vary across QC vendors. For example, IBM devices

currently have the CNOT as the native two-qubit gate [17], Rigetti implement both CZ and iSWAP gates [18, 31], and Google support CZ, SYC, \sqrt{i} SWAP gates [16, 32]. High-level quantum circuits need to be decomposed into the given gate set by using analytical algorithms [33, 34] or numerical approaches [35, 36]. Furthermore, two-qubit gates can only be executed on the connected (nearest neighbouring, NN) qubits. Movement operations such as SWAP gates need to be inserted for performing non-NN gates, increasing the number of gates and circuit depth. However, NISQ computers have limited qubit coherence time and high gate error rates. It is crucial to minimize circuit sizes for reliable implementation of quantum applications. To this purpose, quantum compilation techniques, including qubit mapping and routing, gate decomposition and scheduling, have been developed to efficiently transform high-level quantum circuits into hardware-compatible ones. For general quantum circuits, the routing and scheduling algorithms assign dependencies between gates to maintain the correctness of program semantics [19, 20]. These dependencies are typically generated based on the gate order in an input circuit. These general-purpose quantum compilers work at the gate level can provide efficient compilation. However, most of them do not consider application-level semantics. Any *application-specific* optimizations that can improve application performance are desirable for NISQ computing.

Compilation for Hamiltonian simulation: As mentioned previously, in Hamiltonian simulation two terms in the sum can be exchanged even they do not commute. This means one is free to use any permutation of the operators in the product formula for a circuit implementation. Such application-level property allows more optimizations for Hamiltonian simulation problems but is not exploited by general-purpose quantum compilers. Figure 3 shows an example of compiling a 6-qubit Hamiltonian circuit to a 2×3 grid architecture. A generic compiler inserts 3 SWAP gates and outputs a 7-depth circuit with 12 two-qubit gates. In contrast, a compiler that considers the flexibility in operator permutation only uses 2 SWAPs. Moreover, these SWAP gates can be combined with other gates in the circuit, further decreasing the gate count and circuit depth (the compiled circuit only has 9 two-qubit gates and depth 5). In this work, we design such an application-specific compiler for 2-local qubit Hamiltonian simulation problems to improve application fidelity.

3. Compilation techniques

In this section, we introduce the proposed compilation techniques for quantum simulation. Figure 2 shows the overview of our 2QAN compiler.

3.1. Qubit mapping

The goal of qubit mapping is to find an optimal qubit initial placement such that the number of qubit moving operations required for implementing all two-qubit gates is minimized. Similar to the approaches in [37, 38, 39], the qubit mapping

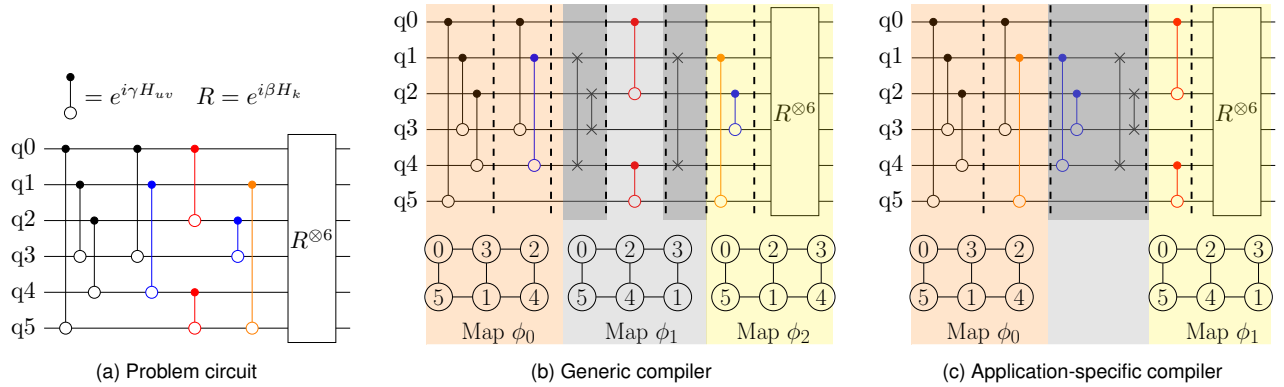


Figure 3: Examples of compiling a 6-qubit 2-local Hamiltonian (Equation 3) to a 3×2 grid architecture. (a) The circuit construction of one Trotter step, where the two(single)-qubit operators implement the evolution of two(single)-qubit Hamiltonians. These two-qubit operators may not commute. (b-c) Compilation procedure. Top figures show the compiled circuits and bottom figures show the qubit mappings (nodes are qubits and edges represent their connectivity). Gates between dashed lines can be performed in parallel. (b) Compilation procedure using a generic compiler that obeys the gate dependencies in (a). For the initial qubit placement (ϕ_0), the first 5 two-qubit gates are directly scheduled. However, the gates on qubit pairs (0,2) and (4,5) are not nearest neighbouring (NN). Two SWAP gates are inserted to route them to be NN (map ϕ_1). To avoid confusion, SWAPs in this Figure are applied on the corresponding hardware qubits, we draw them on the circuit qubits for better readability. Afterwards, another SWAP is added to perform the gate on (1,5) (map ϕ_2). In total, the compiled circuit has 12 two-qubit gates and a depth of 7. (c) Compilation procedure by using a compiler that exploits the flexible operator ordering in Hamiltonian simulation problems. Assuming the same initial map used by the generic compiler, 7 two-qubit gates can be directly scheduled on this map. Then, two SWAP gates are added for performing the gates on (0,2) and (4,5). Moreover, each of these SWAPs can be merged with a circuit unitary, i.e., the circuit in gray area will only have 2 unitaries. In total, the compiled circuit has 9 two-qubit gates and a depth of 5.

problem is formulated as a quadratic assignment problem (QAP). That is, the problem of allocating each qubit in the circuit (facility) to one qubit in the device (location) with the cost defined by a function of the distance and interaction times (flow) between circuit qubits. Let n be the number of circuit qubits or physical qubits and denote by the set $N = \{1, 2, \dots, n\}$. The objective function is

$$\min_{\phi \in S_n} \sum_{i=1}^n \sum_{j=1}^n f_{ij} d_{\phi(i)\phi(j)} \quad (4)$$

where S_n is the set of all permutations $\phi: N \rightarrow N$, f_{ij} is the interaction times between circuit qubits i and j , $d_{\phi(i)\phi(j)}$ is the distance between hardware qubits $\phi(i)$ and $\phi(j)$ and is calculated by using the Floyd-Warshall algorithm.

QAP is a NP-hard problem [40] and we use the Tabu search heuristic algorithm [41, 42] to efficiently find good qubit mappings in this work. Other heuristics such as simulated annealing [43] and greedy randomized adaptive search procedure [44] can be also used for solving this problem. Prior works observed that the QAP formulation of qubit mapping may not work well for general quantum circuits [37, 38, 39]. This is because qubits need to interact in a specific order (gate dependency) and the initial mapping benefits diminish after insertion of SWAPs, e.g., some NN qubits may be moved further apart but will interact later. This is not the case for 2-local Hamiltonian simulation problems as any operator that is NN in a qubit map can be scheduled directly regardless of their order in the

circuit (see examples in Figure 3).

3.2. Qubit routing

Generally, not all two-qubit gates are nearest neighbouring in an initial qubit map. Movement operations such as SWAP gates need to be inserted to move non-NN qubits, causing overheads in gate count and circuit depth. Efficient qubit routing techniques are required to minimize compilation overhead for reliable computation. Different from existing qubit routing algorithms that respect the gate order in the input circuit [20, 23, 45, 46], the routing in 2QAN exploits the operator permutation flexibility in a Hamiltonian. The pseudocode is in Algorithm 1 and an example is shown in Figure 3c.

Given an input circuit that implements one Trotter step of a Hamiltonian, our routing algorithm starts by searching all the two-qubit gates that are NN in an initial qubit layout found by the mapping algorithm (e.g., there are 7 NN two-qubit gates in Figure 3c). These gates are directly mapped and SWAP gates are needed to perform the remaining two-qubit gates (Lines 2-3). For these non-NN gates, it compares their qubit distances in the hardware (the distance matrix in Equation 4) and selects the shortest-distance one to route (Line 5). If there are multiple ones, select the first one in this set. Then the routing algorithm finds all possible SWAP gates on qubits of the chosen gate g (Line 6) It evaluates these SWAPs based on a SWAP selection criteria (will be explained shortly) and selects the best one as the first SWAP for gate g (Line 7). The qubit

map is updated and NN gates are found for the new map and are removed from the un-routed gate set (Lines 8-10). This procedure (Lines 5-10) is repeated until all two-qubit gates are performed. The time complexity of the proposed routing algorithm is $O(gn)$, g is the number of two-qubit gates and n is the number of qubits.

Algorithm 1 Permutation-aware routing

Input: Un-routed circuit, initial map ϕ_0 , device topology
Output: Routed circuit, a set of qubit maps $\{\phi_i\}$ and a set of NN gates corresponding to each map $\{G_{\phi_i}\}$

- 1: Initialize the set of qubit maps $\Phi = \{\phi_0\}$
- 2: Initialize the set of NN gates for each map, $G = \{G_{\phi_0}\}$, $G_{\phi_0} \leftarrow$ all NN two-qubit gates for map ϕ_0
- 3: Initialize $G_{ur} \leftarrow$ all un-routed (non-NN) two-qubit gates
- 4: **while** $G_{ur} \neq \emptyset$ **do**
- 5: Select the gate $g \in G_{ur}$ that has shortest distance in ϕ_i
- 6: $S_g \leftarrow$ Find all SWAP gates on qubits in g
- 7: Select the best SWAP from S_g and add it to G_{ϕ_i}
- 8: Update qubit map from ϕ_i to ϕ_{i+1}
- 9: $G_{\phi_{i+1}} \leftarrow$ Find NN gates in G_{ur} for map ϕ_{i+1}
- 10: Remove all gates in $G_{\phi_{i+1}}$ from G_{ur} , add $G_{\phi_{i+1}}$ to G , add ϕ_{i+1} to Φ
- 11: **end while**

SWAP selection criteria: The best SWAP gate is evaluated based on three criteria:

1. *Least SWAP count:* It will lead to the minimal cost in Equation 4 (i.e., the minimal number of SWAP gates) for remaining non-NN gates.
2. *Shortest circuit depth:* It can be most interleaved with previously mapped gates, introducing the least depth overhead.
3. *Best gate optimization:* It can be merged with a circuit gate. That is, if there is a circuit gate applied on the same qubits as this SWAP, the compiler will replace these two gates by a single gate representing their product (more details will be introduced in the unitary unifying section).

For our compiler configuration, we will evaluate the best SWAP based on the three criteria in the above priority order. Evaluating these criteria in a different order may further improve the compiler but this will not be explored in this work. When there are multiple best options, a random one will be chosen. For example, both SWAP (0,3) and SWAP (2,3) in map ϕ_0 of Figure 3c can be added for performing the two-qubit gate on pair (0,2) and they have the same cost regarding the first two criteria. SWAP (2,3) is selected because it can be combined with a circuit gate that operate on the same qubits. For implementing the circuit gate on pair (4,5), both SWAP (1,5) and SWAP (1,4) are the best, and the compiler randomly selects one.

3.3. Unitary unifying

For each added SWAP gate, the compiler searches over all circuit gates. If there is a circuit gate operating on the same qubit

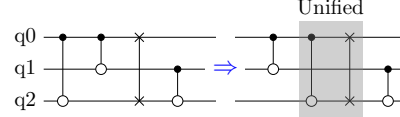


Figure 4: Unitary unifying example. The flexible operator permutation allows the circuit gate on qubits (0,2) to be rescheduled and combined with the SWAP gate.

pair as this SWAP gate, the compiler unifies them into a single gate no matter whether they are consecutive or not (see the example in Figure 4). The unified gate (*dressed SWAP*) is the product of the circuit gate unitary and the SWAP unitary. Such unitary unifying is allowed because of the operator permutation flexibility in Hamiltonian simulation and helps further reduce compilation overhead. Figure 5 shows the decomposition of a SWAP gate, a circuit gate $\exp(i\theta ZZ)$, and their unified unitary into CNOT gates and single-qubit rotations. The unified gate requires 3 CNOTs while the implementation with individual decomposition would require 5 CNOTs in total.

3.4. Gate scheduling

Scheduling without dependency: When connectivity limitations are not considered, the individual exponents for one Trotter step (Equation 1) can be performed in any order. Graph coloring algorithms [47] can be used to schedule such circuits. In the graph construction, nodes represent exponents (gates), and two nodes are connected by an edge if they have common qubits and cannot be scheduled in parallel. We use the default greedy algorithm in NetworkX version 2.5 for our scheduling pass. The circuits, scheduled without taking into account topology constraints, are baseline circuits and will be used for calculating compilation overhead.

Scheduling with dependency: For connectivity-constrained quantum computers, the routing pass in previous section will be applied. The router outputs a list of qubit maps and a set of NN gates corresponding to each map, including both circuit gates and (dressed) SWAP gates. The order of a (dressed) SWAP gate and a circuit gate cannot be exchanged if the SWAP is inserted to make the circuit gate NN. One can generate a gate dependency graph based on the gate order after qubit routing and apply conventional scheduling algorithms [20, 21] to minimize circuit depth (decoherence limit). This approach may perform sufficiently well for some circuits such as the one in Figure 3c, but more optimizations can be achieved for other circuits by considering the operator permutation in Hamiltonian simulation. In this work, we apply such application-specific optimizations and the pseudocode of the proposed gate scheduling algorithm is presented in Algorithm 2 and an example is shown in Figure 6.

Hybrid scheduling: Algorithm 2 is a hybrid of the above two scheduling techniques. The flexible operator permutation property implies that circuit gates can be scheduled in any qubit map where they are NN. The NN circuit gates in

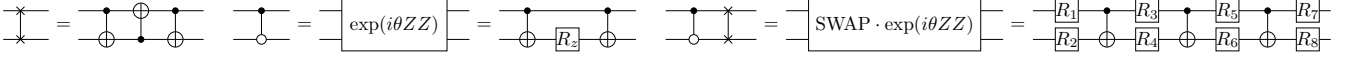


Figure 5: Examples of decomposing the SWAP, the unitary $\exp(i\theta ZZ)$, and their product into CNOTs and single-qubit rotations.

Algorithm 2 Permutation-aware scheduling

Input: The set of maps $\Phi = \{\phi_i\}$ and the set of NN gates corresponding to each map $G = \{G_{\phi_i}\}$

Output: Scheduled circuit

- 1: Use graph coloring algorithm to schedule gates in G_{ϕ_0}
- 2: Initialize scheduling cycle $t = 0$ and the set of scheduled gates in this cycle $C_t = \emptyset$
- 3: Initialize qubit map for cycle t : $M_t \leftarrow$ last map in Φ (for an ALAP scheduling)
- 4: $G_{\text{us}} \leftarrow$ All un-scheduled gates $\in G$
- 5: **while** $G_{\text{us}} \neq \emptyset$ **do**
- 6: **for each** circuit gate $g \in G_{\text{us}}$ **do**
- 7: Schedule g in C_t iff it is NN in M_t and its qubits are free
- 8: **end for**
- 9: **for each** SWAP gate $\in G_{\text{us}}$ **do**
- 10: Schedule it in C_t iff it is NN in M_t , its qubits are free, and there is no dependency violation
- 11: $M_{t+1} \leftarrow$ the map after applying this SWAP on M_t
- 12: **end for**
- 13: $t \leftarrow t + 1$ and update G_{us}
- 14: **end while**
- 15: Reverse the gate sequence in $\{C_0, \dots, C_t\}$ (ALAP)

the initial qubit map do not have dependencies and are first scheduled using the graph coloring algorithm (Line 1). For other qubit maps, dependencies between SWAP and circuit gates need to be respected. The algorithm initializes the circuit cycle $t = 0$. We implement an as-late-as-possible (ALAP) schedule in this work so the algorithm assigns the last qubit map to cycle 0 (M_0 , Line 2). For cycle t , it first finds all circuit gates that can be scheduled (Lines 6-8). A circuit gate can be scheduled at t only if its qubits are NN in map M_t and these qubits are not currently occupied by any other gates. For example, the gate on (1,3) in Figure 6b is scheduled at cycle 0 while it needs to be scheduled at a different cycle in Figure 6a because of the dependency constraint when using a generic scheduler. Afterwards, the scheduler finds all SWAP gates that can be scheduled at this cycle (Lines 9-12). Except the NN and availability requirements, a SWAP gate can be scheduled at t only if the circuit gates that depends on it have been scheduled (e.g., red gates depend on the two SWAPs in Figure 6b). Once a SWAP is inserted, the qubit map for next cycle will be updated. The procedure in Lines 6-13 is repeated until all gates are scheduled. Finally, the algorithm reverses the scheduled gate sequence (Line 15). The time complexity of this hybrid scheduling algorithm scales quadratically with the number of gates.

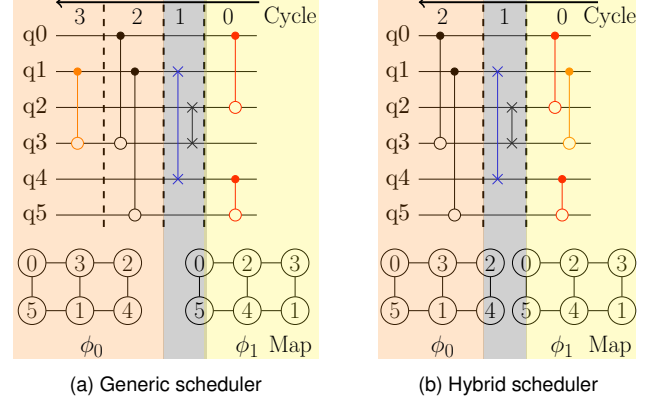


Figure 6: ALAP scheduling examples. (a) A generic scheduler respects the gate order provided by the routing pass. The scheduled circuit takes 4 cycles. (b) The hybrid scheduler considers the flexibility of permuting circuit gates and respects the dependency between a SWAP gate and its corresponding NN circuit gates. For example, it schedules gate on pair (1,3) at cycle 0 because it is a NN circuit gate in map ϕ_1 while a generic scheduler will not schedule it until its predecessor (gate on (1,5)) is performed. This permutation-aware scheduling helps reduce circuit depth and the scheduled circuit takes 3 cycles.

4. Experimental setup

Benchmarks: We consider two 2-local Hamiltonian models, the transverse Ising model

$$H = \sum_{(u,v) \in E} \gamma_{uv} ZZ_{uv} + \sum_{k \in V} \beta_k X_k \quad (5)$$

and the Heisenberg model

$$H = \sum_{(u,v) \in E} (\alpha_{uv} XX_{uv} + \beta_{uv} YY_{uv} + \gamma_{uv} ZZ_{uv}). \quad (6)$$

X, Y, Z are the Pauli operators and the problem graph is described by $G(V, E)$. These are important models in the study of many-body Physics. The computational complexity of computing important properties such as their ground state energy depends on the properties of the graph. Famously, it was shown by Barahona [48] that computing the ground state of a three-dimensional Ising lattice is NP-hard, whereas polynomial classical algorithms are known for the two-dimensional Ising model in the absence of a magnetic field [49].

In our evaluation, we generate the Hamiltonians in a linear array with nearest neighbouring (NN) and next nearest neighbouring (NNN) interactions for both models, they are noted as **NNN Ising** and **NNN Heisenberg**. The time evolution of a Hamiltonian is implemented by using the product formula $(\prod_{j=1}^L \exp(ih_j H_j t/r))^r$, r is the number of Trotter steps and

circuits in different steps are the same. The coefficients of H_j are randomly sampled from $(0, \pi)$. The number of two-qubit operators for NNN Ising and NNN Heisenberg models in each Trotter step is $2n - 3$, n is the number of qubits ranging from 6 to 50 in our evaluation.

In addition, we also use the quantum approximate optimization algorithm (**QAOA**) [25] for solving the MAX-CUT problems on 3-regular graphs as our benchmark. QAOA is a popular benchmark for testing the performance of quantum computers and has been demonstrated in different quantum processors [50, 51]. In particular, the connectivity differs for each problem graph, which is well suited for evaluating compilation techniques. QAOA has the same form as the Ising model, its problem Hamiltonian is $C = \sum_{(u,v) \in E} ZZ_{uv}$ and drive Hamiltonian is $B = \sum_{k \in V} X_k$. The circuit implementation of one-layer QAOA is

$$U(\gamma, \beta) = \prod_{(u,v) \in E} \exp(i\gamma ZZ_{uv}) \prod_{k \in V} \exp(i\beta X_k). \quad (7)$$

Different from Hamiltonian simulation, these operator parameters (γ, β) differ in every layer. In our evaluation, we randomly sample 10 instances of 3-regular graphs. The operator parameters for each instance are chosen at their theoretically optimal values and are calculated by using tools provided in ReCirq [52]. The number of two-qubit operators in one-layer QAOA is $3n/2$, we consider qubit numbers n from 4 to 22.

Quantum computers: We compile these benchmarks onto three quantum computers, **Google Sycamore** [16], **IBMQ Montreal** [17], **Rigetti Aspen** [18]. As shown in Figure 1, Sycamore has a grid architecture with SYC as hardware two-qubit gate, Montreal has a dodecagon lattice with CNOT as native gate, Aspen has connected octagons and iSWAP as native gate. All three devices support arbitrary single-qubit rotations. Experiments on Montreal were performed on 27th June, 2021, the average CNOT error rate was 0.9865%, average read-out error rate was 1.783%, and average T1=104.37 μ s and T2=87.94 μ s.

Quantum compilers: We compare our **2QAN** compiler with two state-of-the-art industrial compilers, the **t|ket** compiler version 0.11.0 [26] and the **Qiskit** compiler version 0.26.2 with optimization level 3 [27]. We use t|ket with the recommended ‘FullPass’ (FullPeepholeOptimise, followed by the default qubit mapping pass, SynthesiseIBM). For circuits with larger number of qubits, the default mapping in t|ket may fail to find a qubit initial placement and we use their ‘LinePlacement’ pass instead. t|ket and Qiskit have advanced circuit optimizations for the CNOT or CZ gates. For devices that have different hardware two-qubit gates, we disable the gate decomposition pass in Qiskit and t|ket. The 2QAN compiler always performs circuit mapping before gate decomposition. The mapped circuits that have application-level unitaries (by Qiskit, t|ket, 2QAN) will need to be decomposed into hardware gate sets. We apply the ‘SynthesiseIBM’ decomposition pass in t|ket to decompose the mapped circuits by 2QAN for

the Montreal device. We use the analytical method in Cirq [53] to decompose QAOA and Ising unitaries into SYC gates. For other application unitaries and hardware gates, we use the numerical approach developed in [36] for finding more efficient decomposition. Both Qiskit and 2QAN involve randomization in the mapping procedure, we run their mapping passes 5 times and choose the best results.

Metrics: Similar to prior works, we use the **number of inserted SWAP gates** (smaller is better), the **number of hardware two-qubit gates** (smaller is better), and the **depth of two-qubit gates** (shorter is better) as metrics to compare the performance of different compilers. We also calculate the increase in gate count and circuit depth (i.e., **compilation overhead**, less is better) compared to the circuits without considering connectivity constraints. Furthermore, we experimentally evaluate the application performance of QAOA benchmarks on the Montreal device. The performance is measured by the **normalized cost function** $\langle C \rangle / C_{\min}$ (larger is better). 1 means the perfect result and 0 corresponds to the random guessing result, more details can be found in [51].

Implementation: We implement 2QAN in Python 3.8. All compilation in our evaluation was performed on a laptop with an Intel Core i7 processor (2.30GHz and 32GB RAM).

5. Compiler evaluation

5.1. Reducing compilation overhead

In this section, we compare the compilation overhead of our 2QAN compiler with Qiskit and t|ket. Figures 7, 8, 9 show the compilation results on Google Sycamore, Rigetti Aspen, and IBM Montreal, respectively. Compared to t|ket and Qiskit, 2QAN has least compilation overhead in terms of the number of inserted SWAP gates, the number of hardware two-qubit gates, and the circuit depth. We summarize the overhead reduction of 2QAN versus t|ket and Qiskit in Tables 1 and 2 respectively. The reduction is calculated by the overhead of t|ket or Qiskit divided by the overhead of 2QAN.

Reducing SWAP count: 2QAN exploits the term permutation flexibility in Hamiltonian simulation and inserts *least number of SWAP gates* compared to Qiskit and t|ket across all benchmarks and quantum computers. For example, when compiling quantum applications to the Sycamore device, 2QAN inserts on average 1.7x fewer SWAPs than t|ket and 6x fewer than Qiskit for the Heisenberg model. The number of inserted SWAPs for the Ising model is similar to the Heisenberg model because they require the same qubit connectivity. For QAOA benchmarks, 2QAN inserts on average 1.8x fewer SWAPs than t|ket and 4.7x fewer than Qiskit. For the Aspen device, across three benchmarks, the maximum SWAP reduction relative to t|ket and Qiskit is around 2.4x and 4.3x, respectively. For the Montreal device, the maximum SWAP reduction across benchmarks compared to t|ket and Qiskit is around 4.6x and 10.1x.

Reducing hardware gate count: The SWAP count reduction

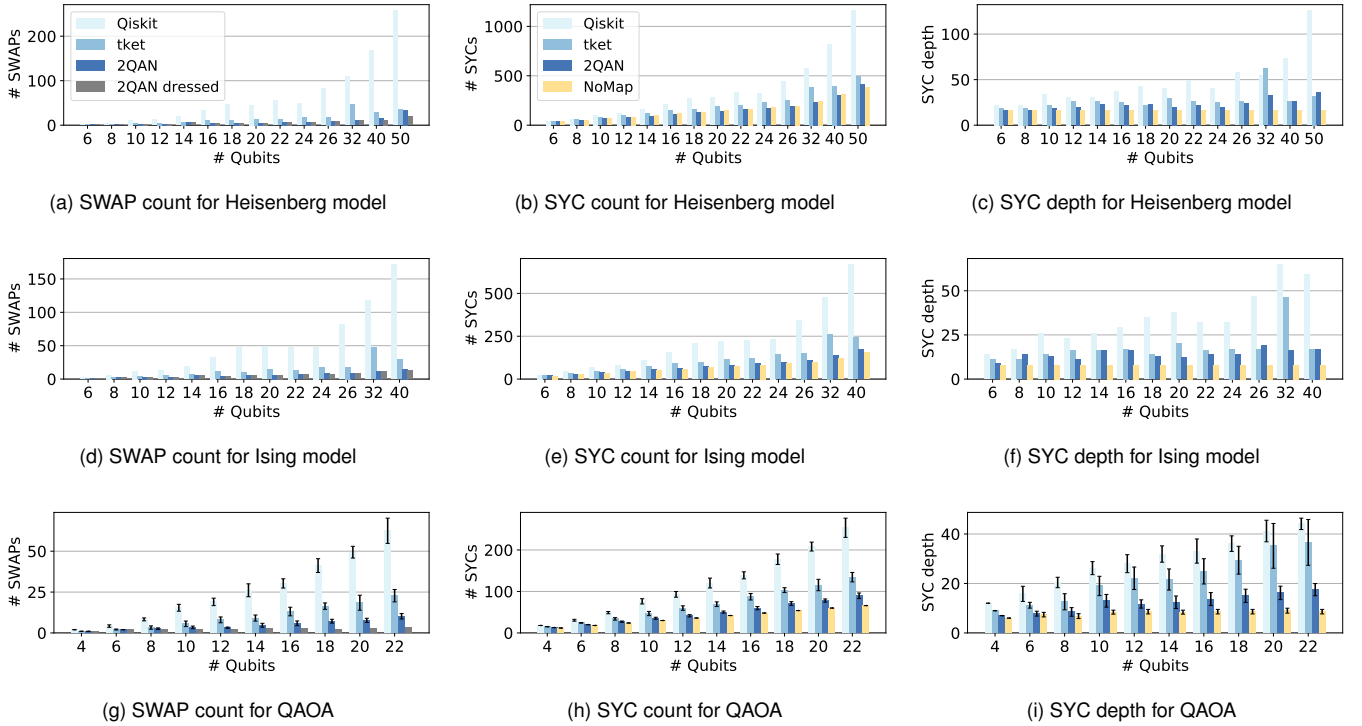


Figure 7: Compilation results of the one-layer NNN Heisenberg model, NNN Ising model, and QAOA on the Google Sycamore device. Each QAOA problem size is averaged over 10 different instances (error bars show the standard deviation) and operator parameters of QAOA circuits were chosen at their theoretically optimal values. ‘2QAN dressed’ shows the number of SWAPs that were merged with circuit gates by 2QAN, which helps to reduce hardware gate count. ‘NoMap’ as our baseline, represents the compilation results when assuming all-to-all qubit connectivity. The 2QAN compiler has least compilation overhead (# SWAPs, # SYCs, and circuit depth) compared to Qiskit and t|ket>.

due to the qubit mapping and routing passes in 2QAN lead to a reduction on hardware gate count. Furthermore, the unitary unifying pass in 2QAN provides further improvements by combining a SWAP gate and a circuit gate into one single gate. The gray bars in (a), (d), (g) of Figures 7-9 show that a large percent of SWAPs can be unified with circuit gates. Across all benchmarks and quantum computers, the circuits compiled by 2QAN have *least number of hardware two-qubit gates* compared to the circuits compiled by Qiskit and t|ket>.

For example, when compiling to the Sycamore device, 2QAN almost has *no SYC overhead* compared to the baseline ‘NoMap’ for the Heisenberg model. This is because most of the SWAPs can be combined with circuit gates (Figure 7a) and such an unified gate can be decomposed into similar number of SYCs as a circuit gate $\exp(it(\alpha XX + \beta YY + \gamma ZZ))$. In contrast, t|ket> and Qiskit lead to on average 24.5% and 92.3% SYC overhead. For the Ising model, 2QAN has on average 8.7% SYC overhead (the circuit unitary $\exp(i\theta ZZ)$ requires fewer SYCs than its combination with SWAP). For the Aspen device, 2QAN reduces iSWAP overhead by up to 5x and 13x compared to t|ket> and Qiskit respectively. For the Montreal device, the maximum CNOT reduction relative to t|ket> and Qiskit is 12.8x and 27.8x respectively.

Reducing circuit depth: The hardware gate count reduction by using the 2QAN compiler leads to reduction in circuit depth. Across all benchmarks and quantum computers, most of the circuits compiled by 2QAN have *shortest depth* compared to the circuits compiled by Qiskit and t|ket>. For the Sycamore device, the maximum depth reduction is 9.5x and 21x with respect to t|ket> and Qiskit respectively. For the Aspen device, 2QAN reduces depth overhead over all benchmarks by on average 1.7x and 3.1x compared to t|ket> and Qiskit. For the Montreal device, the average depth reduction relative to t|ket> and Qiskit is 2.7x and 3.8x.

5.2. Improving application performance

To study how the compilation overhead reduction impacts application performance, we experimentally implemented the QAOA benchmarks with different numbers of layers on the IBMQ Montreal device. For the multiple-layer QAOA circuits, the 2QAN compiler only performs compilation for the first layer and obtains a circuit c_1 . For odd number layers, it directly uses the compiled circuit c_1 . For even number layers, it simply reverses the two-qubit gate order in c_1 . In contrast, t|ket> and Qiskit compile a multiple-layer QAOA circuit as a whole. For all three compilers, the compilation overhead

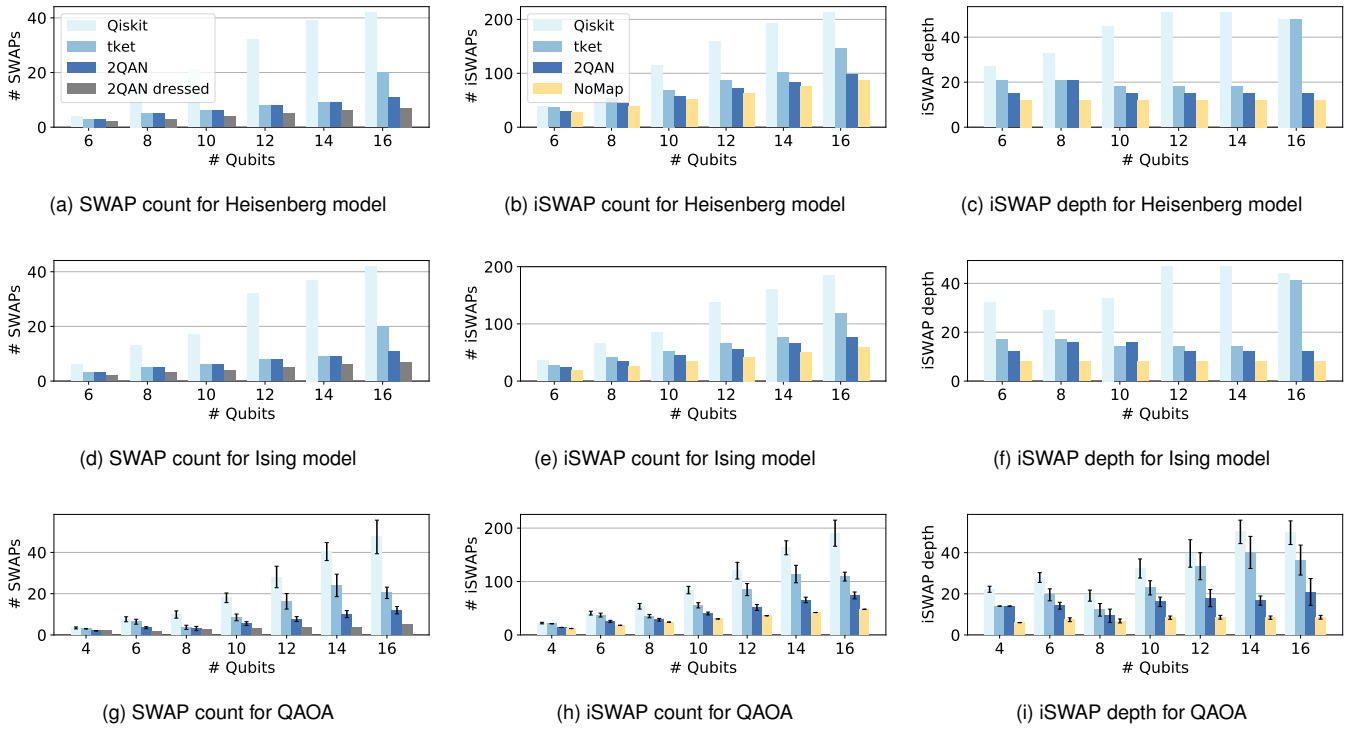


Figure 8: Compilation results of the one-layer NNN Heisenberg model, NNN Ising model, and QAOA on the Rigetti Aspen device. The 2QAN compiler has least compilation overhead (# SWAPs, # iSWAPs, and circuit depth) compared to Qiskit and tket).

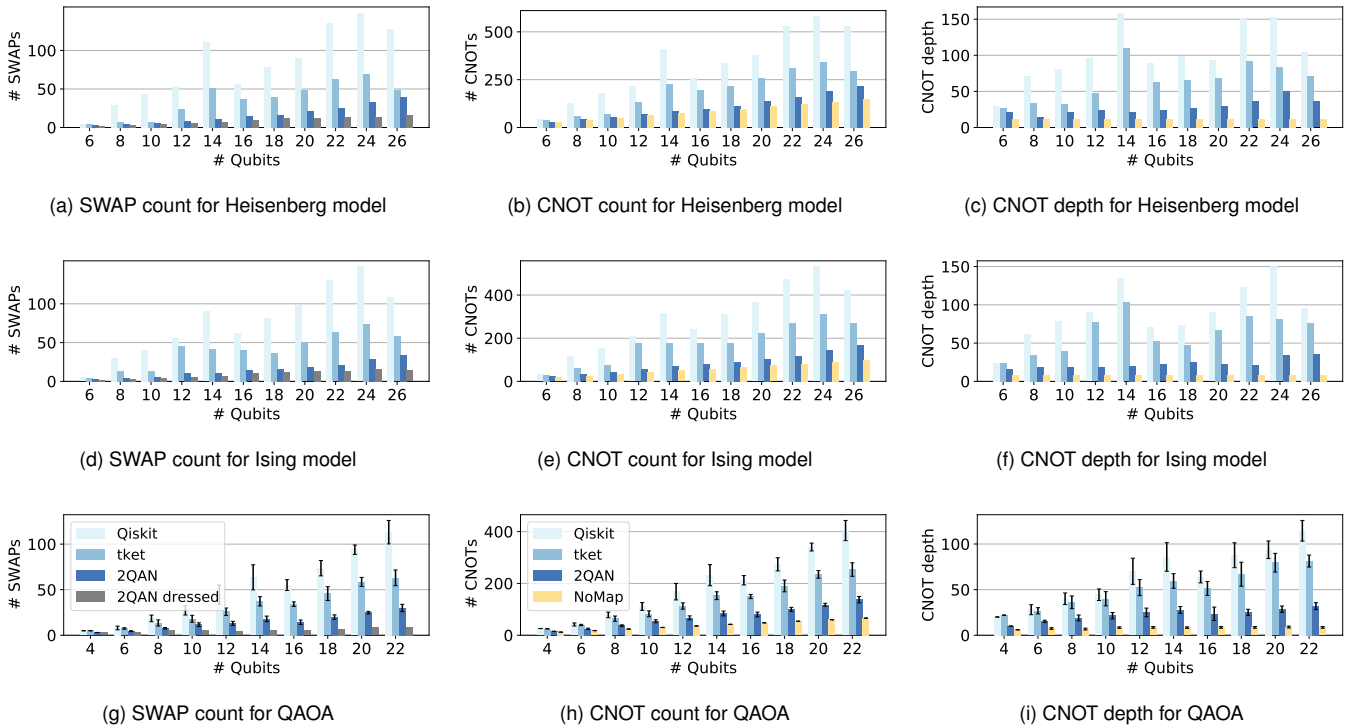


Figure 9: Compilation results of the one-layer NNN Heisenberg model, NNN Ising model, and QAOA on the IBMQ Montreal device. The 2QAN compiler has least compilation overhead (# SWAPs, # CNOTs, and circuit depth) compared to Qiskit and tket).

	Sycamore						Aspen						Montreal					
	SWAPs		SYCs		Depth		SWAPs		iSWAPs		Depth		SWAPs		CNOTs		Depth	
	avg	max	avg	max	avg	max	avg	max	avg	max	avg	max	avg	max	avg	max	avg	max
Heisenberg	1.7x	3.9x	–	–	1.2x	2.7x	1.1x	1.8x	3.2x	5x	1.5x	3.2x	2.2x	4.6x	6x	12.8x	2.4x	5.2x
Ising	1.9x	3.9x	5.6x	10.7x	1.3x	2.9x	1.1x	1.8x	2x	3.2x	1.5x	3.4x	2.7x	4.1x	4.9x	7.8x	2.7x	4x
QAOA	1.8x	2.5x	3.2x	4.4x	3.9x	9.5x	1.8x	2.4x	3x	4.5x	2.2x	3.8x	2x	2.4x	3x	4.3x	3x	4x

Table 1: The average (avg) and maximum (max) compilation overhead reduction when comparing 2QAN with $t|ket\rangle$. For the cases with blank values ‘–’, the 2QAN compiler has negligible overhead.

	Sycamore						Aspen						Montreal					
	SWAPs		SYCs		Depth		SWAPs		iSWAPs		Depth		SWAPs		CNOTs		Depth	
	avg	max	avg	max	avg	max	avg	max	avg	max	avg	max	avg	max	avg	max	avg	max
Heisenberg	6x	9.7x	–	–	1.8x	2.6x	3.3x	4.3x	9.3x	13x	2.7x	3.4x	5.1x	10.1x	14x	27.8x	3.8x	7.6x
Ising	6.7x	11.5x	19x	30.7x	2.4x	4.1x	3.3x	4.1x	5.6x	7.4x	3x	3.9x	5.3x	8.2x	9.7x	15x	4x	7.4x
QAOA	4.7x	6.4x	8x	10.6x	6.9x	21x	3.1x	4x	5.2x	6.9x	3.5x	5x	3x	3.9x	4.4x	5.1x	3.7x	4.8x

Table 2: The average (avg) and maximum (max) compilation overhead reduction when comparing 2QAN with Qiskit. For the cases with blank values ‘–’, the 2QAN compiler has negligible overhead.

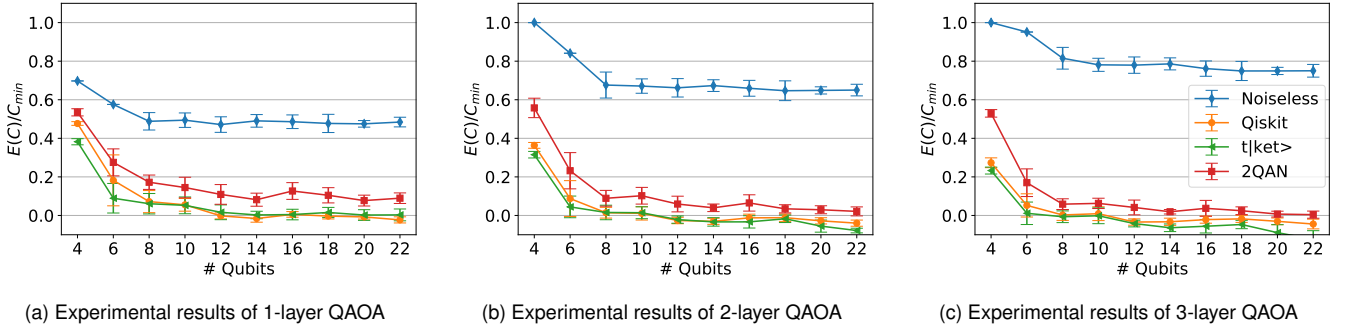


Figure 10: Experimental results of running QAOA on the IBMQ Montreal device. The y axis shows the application performance, which is measured by the normalized cost function $\langle C \rangle / C_{\min}$ (larger is better). Each problem size is averaged over 10 different instances (error bars show the standard deviation). The operator parameters of QAOA circuits were chosen at their theoretically optimal values. For the same layer QAOA, 2QAN always achieves better application performance compared to both Qiskit and $t|ket\rangle$. The ideal costs increase with the number of QAOA layers (noiseless results in (a-c)). However, in experimental implementation increasing QAOA layers (increasing circuit sizes) increases the probabilities of hardware errors. For the Montreal device, only the performance of the 4-qubit QAOA compiled by 2QAN improves when the layer is increased from 1 to 2.

of a n -layer QAOA circuit is approximately n times of the overhead of a single-layer circuit (see Figure 11 in the Appendix). For quantum applications in NISQ computers, the implementation that has fewer hardware gates (reducing gate errors) and shorter circuit depth (reducing decoherence errors) should have better performance (higher fidelity). This is experimentally demonstrated in Figure 10, the circuits compiled by our 2QAN compiler have the *best application performance* compared to the results from using $t|ket\rangle$ and Qiskit for all problem sizes and all QAOA layers.

For example, as noise accumulates in QAOA circuits they will often converge to the value 0 corresponding to a random guess. Here we see that the 3-layer QAOA benchmarks compiled by either $t|ket\rangle$ or Qiskit already approach zero for problems with 8 qubits. In comparison, 2QAN only comes close to this value for much larger problems (around 20 qubits). Ideally (without hardware noise), the application performance

should improve with the number of QAOA layers. However, in practice there is a trade off, with additional layers also increasing the overall error probabilities, and hence decreasing application performance. Figure 10 shows that the QAOA performance of all problem sizes decreases when the number of layers increases for all three compilers except the 4-qubit QAOA compiled by 2QAN of which performance improves when increasing the layer number from 1 to 2. This implies that efficient compilation techniques can enhance device capacity and potentially pave the way towards practical applications of quantum computing.

5.3. Scalability and runtime

We use the Tabu search algorithm for solving the qubit placement problem. This algorithm is fast for solving small problems, e.g, it takes around 1.6 seconds for the 10-qubit Ising model and 12.2 seconds for the 20-qubit QAOA. However,

it becomes slow for larger problems and takes 330.2 (976.3) seconds for the 40(50)-qubit Heisenberg model. Qubit placement is not our main optimization goal in this work. More efficient algorithms exist for solving QAP problems [54] and other qubit mapping techniques [26, 27] could also be applied in future work. The proposed routing and scheduling heuristics (Algorithm 1 and Algorithm 2) scale linearly and quadratically with the number of gates in one Trotter step. Moreover, we only perform the compilation for the first Trotter step and simply use this circuit for odd-number steps and reverse the two-qubit gate order for even-number steps. Such an implementation saves compilation time and is similar to the second-order Trotterization in Equation 2. The runtime evaluation and scalability analysis give us confidence that the 2QAN compiler will scale up to near-term quantum applications with a considerable number of qubits and gates.

6. Related work

The product formula is the most established approach to simulate the dynamics of quantum systems. Approximation errors arise when there are anti-commuting terms in the Hamiltonian. To achieve a desired precision, the time evolution is divided into many small time steps. Assume a simulation circuit has r Trotter steps and the gate count for implementing each step is G . Minimizing the circuit size (Gr) meanwhile maintaining computational accuracy is crucial for a practical implementation. Childs et al. show that randomly permuting the Hamiltonian terms can lead to implementations with fewer Trotter steps compared to the method that fixing the term order [29]. Campbell presents another protocol that randomly samples each term with a probability proportional to its strength in the Hamiltonian [30]. Both analytical and numerical results show that this stochastic protocol can effectively reduce circuit size. Since then several improved algorithms based on randomization have also been proposed [55, 56, 57].

Besides the improvement on high-level circuit construction, some works focus on optimizing the low-level circuit (i.e., decomposed circuit with only hardware gates) for each Trotter step. van den Berg et al. [58] and Cowtan et al. [59] optimize the circuits by applying simultaneous diagonalization of Pauli exponentials. Others present circuit synthesis method based on the ZX-calculus [60, 61]. However, these works are restricted to CNOT or CZ gates and may not be applicable (or cause high overhead) for quantum computers with other hardware gates such as SYC and iSWAP. Moreover, most of them do not take the qubit connectivity constraint into account and therefore require further compilation.

Many compilation techniques have been proposed to map quantum circuits onto NISQ computers. Some of them optimize gate count to reduce high probability errors from two-qubit gates or minimize circuit depth to mitigate the effect of decoherence [19, 20, 21, 22]. Others consider spatial and temporal noise variations and develop noise-aware compilation algorithms to minimize error rates [23, 24, 45, 62]. Indus-

trial quantum compilers such as tket [26] and Qiskit [27] incorporate multiple techniques to achieve the best application performance. These general-purpose compilers typically operate at the gate level and can work for general quantum applications. However, they have little knowledge of the mathematical properties at the application level and therefore lack fine-grained optimizations. Application-specific compilation techniques will be advantageous for NISQ computing. For example, tailored gate decomposition and qubit architecture for the Fermi-Hubbard model can provide a more efficient simulation [63]. Specialized compilers for variational quantum algorithms can significantly reduce the compilation overhead [64] and compilation runtime [65].

This work discovered the compiler optimization opportunity based on the flexible term permutation property in the product formula approach for quantum simulation problems. Exploiting this flexibility, we presented application-specific algorithms to minimize compilation overhead. Our 2QAN compiler can target different architectures and provide efficient compilation for different gate sets. Conventional compilation techniques may not be adapted to this application property, because 1) the application-level commutativity is difficult to be recognized by the gate-level optimization and 2) many terms in the Hamiltonian do not commute and changing the order of anti-commuting gates will be prohibited.

7. Conclusions

We have developed an application-specific compiler for 2-local qubit Hamiltonian simulation problems. The designed 2QAN compiler exploits the flexibility of permuting operators in a Hamiltonian and performs optimizations on the qubit routing, gate synthesis, and gate scheduling passes. Evaluation results showed that 2QAN can significantly reduce compilation overhead compared to two industrial compilers across three benchmarks and three quantum computers. For some applications, 2QAN even has no gate overhead. Furthermore, experimental results demonstrated that 2QAN can achieve the highest application fidelity in practice on hardware. We believe application-specific compilation techniques will help enhance the performance of quantum applications on NISQ devices and allow them to explore their maximum capacities.

This is the first attempt to incorporate the flexible operator permutation property of Hamiltonian simulation problems into the qubit routing and gate scheduling passes. More optimizations may be performed and other research directions can be investigated. First, the objective of 2QAN is to minimize the number of SWAP gates and circuit depth. NISQ computers have inhomogeneities and noise-aware compilation techniques can be used to maximize application fidelity [23, 24, 45, 62]. Furthermore, error mitigation techniques can be applied to further reduce errors [66, 67, 68, 69]. In the experimental results reported here, we only compiled the first Trotter step in Hamiltonian simulation and simply applied a reverse scheduling for the two-qubit gates in the even-number steps. Prior works

prove that randomizing the operator order in each step can reduce the simulation costs [29, 30]. Future work can adapt 2QAN to this randomization and also analyze how randomized compiling affects approximation errors and the efficiency of quantum simulation algorithms. In addition, it is worthwhile to investigate how to generalize these compilation techniques for k -local Hamiltonians.

Acknowledgements

We thank Silas Dilkes for help with the `t|ket` compiler. We thank César A. Rodríguez Rosario for help with the experimental setup on the IBMQ Montreal device via StrangeWorks QC platform. We acknowledge use of the IBM Q for this work. We acknowledge funding from the EPSRC Prosperity Partnership in Quantum Software for Modelling and Simulation (Grant No. EP/S005021/1).

References

- [1] Sadeqh Raeisi, Nathan Wiebe, and Barry C Sanders. Quantum-circuit design for efficient simulations of many-body quantum dynamics. *New Journal of Physics*, 14(10):103017, 2012.
- [2] David Poulin, Matthew B Hastings, Dave Wecker, Nathan Wiebe, Andrew C Doherty, and Matthias Troyer. The Trotter step size required for accurate quantum simulation of quantum chemistry. *arXiv preprint arXiv:1406.4920*, 2014.
- [3] Stephen P Jordan, Keith SM Lee, and John Preskill. Quantum algorithms for quantum field theories. *Science*, 336(6085):1130–1133, 2012.
- [4] Cornelius Hempel, Christine Maier, Jonathan Romero, Jarrod McClean, Thomas Monz, Heng Shen, Petar Jurcevic, Ben P Lanyon, Peter Love, Ryan Babbush, et al. Quantum chemistry calculations on a trapped-ion quantum simulator. *Physical Review X*, 8(3):031022, 2018.
- [5] Frank Arute, Kunal Arya, Ryan Babbush, Dave Bacon, Joseph C Bardin, Rami Barends, Andreas Bengtsson, Sergio Boixo, Michael Broughton, Bob B Buckley, David A Buell, Brian Burkett, Nicholas Bushnell, Yu Chen, Zijun Chen, Yu-An Chen, Ben Chiaro, Roberto Collins, Stephen J Cotton, William Courtney, Sean Demura, Alan Derk, Andrew Dunsworth, Daniel Eppens, Thomas Ekl, Catherine Erickson, Edward Farhi, Austin Fowler, Brooks Foxen, Craig Gidney, Marissa Giustina, Rob Graff, Jonathan A Gross, Steve Habegger, Matthew P Harrigan, Alan Ho, Sabrina Hong, Trent Huang, William Huggins, Lev B Ioffe, Sergei V Isakov, Evan Jeffrey, Zhang Jiang, Cody Jones, Dvir Kafri, Kostyantyn Kechedzhi, Julian Kelly, Seon Kim, Paul V Klimov, Alexander N Korotkov, Fedor Kostritsa, David Landhuis, Pavel Laptev, Mike Lucero, Erik Lucero, Michael Marthaler, Orion Martin, John M Martinis, Anika Marusczyk, Sam McArdle, Jarrod R McClean, Trevor McCourt, Matt McEwen, Anthony Megrant, Carlos Mejuto-Zaera, Xiao Mi, Masoud Mohseni, Wojciech Mruczkiewicz, Josh Mutus, Ofer Naaman, Matthew Neeley, Charles Neill, Hartmut Neven, Michael Newman, Murphy Yuezhen Niu, Thomas E O’Brien, Eric Ostby, Bálint Pató, Andre Petukhov, Harald Putterman, Chris Quintana, Jan-Michael Reiner, Pedram Roushan, Nicholas C Rubin, Daniel Sank, Kevin J Satzinger, Vadim Smelyanskiy, Doug Strain, Kevin J Sung, Peter Schmitteckert, Marco Szalay, Norm M Tubman, Amit Vainsencher, Theodore White, Nicolas Vogt, Z Jamie Yao, Ping Yeh, Adam Zalcman, and Sebastian Zanker. Observation of separated dynamics of charge and spin in the Fermi-Hubbard model. *arXiv preprint arXiv:2010.07965*, October 2020.
- [6] Iulia M Georgescu, Sahel Ashhab, and Franco Nori. Quantum simulation. *Reviews of Modern Physics*, 86(1):153, 2014.
- [7] Richard P Feynman. Simulating physics with computers. *International Journal of Theoretical Physics*, 21(6/7), 1982.
- [8] Hale F Trotter. On the product of semi-groups of operators. *Proceedings of the American Mathematical Society*, 10(4):545–551, 1959.
- [9] Seth Lloyd. Universal quantum simulators. *Science*, pages 1073–1078, 1996.
- [10] Dominic W Berry, Andrew M Childs, Richard Cleve, Robin Kothari, and Rolando D Somma. Simulating hamiltonian dynamics with a truncated taylor series. *Physical review letters*, 114(9):090502, 2015.
- [11] Dominic W Berry and Andrew M Childs. Black-box hamiltonian simulation and unitary implementation. *Quantum Information & Computation*, 12(1-2):29–62, 2012.
- [12] Guang Hao Low and Isaac L Chuang. Optimal hamiltonian simulation by quantum signal processing. *Physical review letters*, 118(1):010501, 2017.
- [13] Ryan Babbush, Jarrod McClean, Dave Wecker, Alán Aspuru-Guzik, and Nathan Wiebe. Chemical basis of Trotter-Suzuki errors in quantum chemistry simulation. *Physical Review A*, 91(2):022311, 2015.
- [14] Andrew M Childs, Dmitri Maslov, Yunseong Nam, Neil J Ross, and Yuan Su. Toward the first quantum simulation with quantum speedup. *Proceedings of the National Academy of Sciences*, 115(38):9456–9461, 2018.
- [15] John Preskill. Quantum computing in the nisq era and beyond. *Quantum*, 2:79, 2018.
- [16] Frank Arute, Kunal Arya, Ryan Babbush, Dave Bacon, Joseph C Bardin, Rami Barends, Rupak Biswas, Sergio Boixo, Fernando G S L Brandao, David A Buell, Brian Burkett, Yu Chen, Zijun Chen, Ben Chiaro, Roberto Collins, William Courtney, Andrew Dunsworth, Edward Farhi, Brooks Foxen, Austin Fowler, Craig Gidney, Marissa Giustina, Rob Graff, Keith Guerin, Steve Habegger, Matthew P Harrigan, Michael J Hartmann, Alan Ho, Markus Hoffmann, Trent Huang, Travis S Humble, Sergei V Isakov, Evan Jeffrey, Zhang Jiang, Dvir Kafri, Kostyantyn Kechedzhi, Julian Kelly, Paul V Klimov, Sergey Knysh, Alexander Korotkov, Fedor Kostritsa, David Landhuis, Mike Lindmark, Erik Lucero, Dmitri Lyakh, Salvatore Mandrà, Jarrod R McClean, Matthew McEwen, Anthony Megrant, Xiao Mi, Kristel Michielsen, Masoud Mohseni, Josh Mutus, Ofer Naaman, Matthew Neeley, Charles Neill, Murphy Yuezhen Niu, Eric Ostby, Andre Petukhov, John C Platt, Chris Quintana, Eleanor G Rieffel, Pedram Roushan, Nicholas C Rubin, Daniel Sank, Kevin J Satzinger, Vadim Smelyanskiy, Kevin J Sung, Matthew D Trevischio, Amit Vainsencher, Benjamin Villalonga, Theodore White, Z Jamie Yao, Ping Yeh, Adam Zalcman, Hartmut Neven, and John M. Martinis. Quantum supremacy using a programmable superconducting processor. *Nature*, 574(7779):505–510, 2019.
- [17] IBM. IBM Quantum Experience Devices. <https://quantum-computing.ibm.com/>, 2020.
- [18] Rigetti. Rigetti computing. <https://www.rigetti.com/>, 2020.
- [19] Alwin Zulehner, Alexandru Paler, and Robert Wille. An efficient methodology for mapping quantum circuits to the IBM QX architectures. *IEEE Transactions on Computer-Aided Design of Integrated Circuits and Systems*, 38(7):1226–1236, 2018.
- [20] Alexander Cowtan, Silas Dilkes, Ross Duncan, Alexandre Krajenbrink, Will Simmons, and Seyon Sivarajah. On the qubit routing problem. *arXiv preprint arXiv:1902.08091*, 2019.
- [21] Lingling Lao, Hans van Someren, Imran Ashraf, and Carmen G. Almudever. Timing and resource-aware mapping of quantum circuits to superconducting processors. *IEEE Transactions on Computer-Aided Design of Integrated Circuits and Systems*, pages 1–1, 2021.
- [22] Andrew M Childs, Eddie Schoute, and Cem M Unsal. Circuit transformations for quantum architectures. *arXiv preprint arXiv:1902.09102*, 2019.
- [23] Gushu Li, Yufei Ding, and Yuan Xie. Tackling the qubit mapping problem for NISQ-era quantum devices. In *Proceedings of the Twenty-Fourth International Conference on Architectural Support for Programming Languages and Operating Systems*, pages 1001–1014. ACM, 2019.
- [24] Prakash Murali, Jonathan M Baker, Ali Javadi-Abhari, Frederic T Chong, and Margaret Martonosi. Noise-Adaptive Compiler Mappings for Noisy Intermediate-Scale Quantum Computers. In *Proceedings of the Twenty-Fourth International Conference on Architectural Support for Programming Languages and Operating Systems*, pages 1015–1029, 2019.
- [25] Edward Farhi, Jeffrey Goldstone, and Sam Gutmann. A quantum approximate optimization algorithm. *arXiv:1411.4028*, 2014.
- [26] Seyon Sivarajah, Silas Dilkes, Alexander Cowtan, Will Simmons, Alec Edgington, and Ross Duncan. `t|ket`: a retargetable compiler for NISQ devices. *Quantum Science and Technology*, 6(1):014003, 2020.
- [27] Héctor Abraham, AduOfiei, Rochisha Agarwal, Ismail Yunus Akhaway, Gadi Aleksandrowicz, Thomas Alexander, Eli Arbel, Abraham Asfaw, Carlos Azaustre, AzizNgoueya, Aman Bansal, Panagiotis Barkoutsos, George Barron, Luciano Bello, Yael Ben-Haim, Daniel Bevenius, Lev S. Bishop, Sorin Bolos, Samuel Bosch, Sergey Bravyi, David Bucher, Artemiy Burov, Fran Cabrera, Padraic Calpin, Lauren Capelluto, Jorge Carballo, Ginés Carrascal, Adrian Chen, Chun-Fu Chen, Edward Chen, Jielun (Chris) Chen, Richard Chen, Jerry M. Chow, Spencer Churchill, Christian Claus, Christian Clauss, Romilly

- Cocking, Abigail J. Cross, Andrew W. Cross, Simon Cross, Juan Cruz-Benito, Chris Culver, Antonio D. Córcoles-Gonzales, Sean Dague, Tareq El Dandachi, Marcus Daniels, Matthieu Dartiailh, Davide Ferr, Abdón Rodríguez Davila, Anton Dekusar, Delton Ding, Jun Doi, Eric Drechsler, Drew, Eugene Dumitrescu, Karel Dumon, Ivan Duran, Kareem EL-Safty, Eric Eastman, Pieter Eendebak, Daniel Egger, Mark Everitt, Paco Martín Fernández, Axel Hernández Ferrera, Romain Fouilland, Franck Chevallier, Albert Frisch, Andreas Fuhrer, MELVIN GEORGE, Julien Gacon, Borja Godoy Gago, Claudio Gambella, Jay M. Gambetta, Adhisha Gammanpila, Luis Garcia, Shelly Garion, Austin Gilliam, Aditya Giridharan, Juan Gomez-Mosquera, Salvador de la Puente González, Jesse Gorzinski, Ian Gould, Donny Greenberg, Dmitry Grinko, Wen Guan, John A. Gunnels, Mikael Haglund, Isabel Haide, Ikko Hamamura, Omar Costa Hamido, Vojtech Havlicek, Joe Hellmers, Łukasz Herok, Stefan Hillmich, Hiroshi Horii, Connor Howington, Shaohan Hu, Wei Hu, Rolf Huisman, Haruki Imai, Takashi Imamichi, Kazuaki Ishizaki, Raban Iten, Toshihiko Itoko, James Seaward, Ali Javadi, Ali Javadi-Abhari, Jessica, Madhav Jivrajani, Kiran Johns, Jonathan-Shoemaker, Tal Kachmann, Naoki Kanazawa, Kang-Bae, Anton Karazeev, Paul Kassebaum, Spencer King, Knabberjoe, Yuri Kobayashi, Arseny Kovyrshin, Rajiv Krishnakumar, Vivek Krishnan, Kevin Krsulich, Gawel Kus, Ryan LaRose, Enrique Lacal, Raphaël Lambert, John Lapeyre, Joe Latone, Scott Lawrence, Christina Lee, Gushu Li, Dennis Liu, Peng Liu, Yunho Maeng, Aleksei Malyshev, Joshua Manela, Jakub Mareček, Manuel Marques, Dmitri Maslov, Dolph Mathews, Atsushi Matsuo, Douglas T. McClure, Cameron McGarry, David McKay, Dan McPherson, Srujan Meesala, Thomas Metcalfe, Martin Mevissen, Antonio Mezzacapo, Rohit Midha, Zlatko Minev, Abby Mitchell, Nikolaj Moll, Michael Duane Mooring, Renier Morales, Niall Moran, MrF, Prakash Murali, Jan Müggenburg, David Nadlinger, Ken Nakanishi, Giacomo Nannicini, Paul Nation, Edwin Navarro, Yehuda Naveh, Scott Wyman Neagle, Patrick Neuweiler, Pradeep Niroula, Hassi Norlen, Lee James O’Riordan, Oluwatobi Ogundayo, Pauline Ollitrault, Steven Oud, Dan Padilha, Hanhee Paik, Yuchen Pang, Simone Perriello, Anna Phan, Francesco Piro, Marco Pistoia, Christophe Piveteau, Alejandro Pozas-iKerstjens, Viktor Prutyayov, Daniel Puzzuoli, Jesús Pérez, Quintiii, Rafey Iqbal Rahman, Arun Raja, Nipun Ramagiri, Anirudh Rao, Rudy Raymond, Rafael Martín-Cuevas Redondo, Max Reuter, Julia Rice, Diego M. Rodríguez, Rohith Karur, Max Rossmann, Mingi Ryu, Tharmashastha SAPV, Sam Ferracin, Martin Sandberg, Ritvik Sapra, Hayk Sargsyan, Aniruddha Sarkar, Ninad Sathaye, Bruno Schmitt, Chris Schnabel, Zachary Schoenfeld, Travis L. Scholten, Eddie Schoute, Joachim Schwarm, Ismael Faro Sertage, Kanav Setia, Nathan Shammah, Yunong Shi, Adenilton Silva, Andrea Simonetto, Nick Singstock, Yukio Siraichi, Iskandar Sitdikov, Seyon Sivarajah, Magnus Berg Sletfjerding, John A. Smolin, Mathias Soeken, Igor Olegovich Sokolov, Soolu Thomas, Starfish, Dominik Steenken, Matt Stypulkoski, Shaojun Sun, Kevin J. Sung, Hitomi Takahashi, Ivano Tavernelli, Charles Taylor, Pete Taylour, Soolu Thomas, Mathieu Tillet, Maddy Tod, Miroslav Tomasik, Enrique de la Torre, Kenso Trabing, Matthew Treinish, TrishaPe, Wes Turner, Yotam Vaknin, Carmen Recio Valcarce, Francois Varchon, Almudena Carrera Vazquez, Victor Villar, Desiree Vogt-Lee, Christophe Vuillot, James Weaver, Rafal Wieczorek, Jonathan A. Wildstrom, Erick Winston, Jack J. Woehr, Stefan Woerner, Ryan Woo, Christopher J. Wood, Ryan Wood, Stephen Wood, Steve Wood, James Wootton, Daniyar Yeralin, David Yonge-Mallo, Richard Young, Jessie Yu, Christopher Zachow, Laura Zdanski, Helena Zhang, Christa Zoufal, and Zoufal. Qiskit: An open-source framework for quantum computing, 2019.
- [28] Masuo Suzuki. General theory of fractal path integrals with applications to many-body theories and statistical physics. *Journal of Mathematical Physics*, 32(2):400–407, 1991.
- [29] Andrew M Childs, Aaron Ostrander, and Yuan Su. Faster quantum simulation by randomization. *Quantum*, 3:182, 2019.
- [30] Earl Campbell. Random compiler for fast Hamiltonian simulation. *Physical review letters*, 123(7):070503, 2019.
- [31] Deanna M Abrams, Nicolas Didier, Blake R Johnson, Marcus P da Silva, and Colm A Ryan. Implementation of the XY interaction family with calibration of a single pulse. *arXiv preprint arXiv:1912.04424*, 2019.
- [32] B. Foxen, C. Neill, A. Dunswoth, P. Roushan, B. Chiaro, A. Megrant, J. Kelly, Zijun Chen, K. Satzinger, R. Barends, F. Arute, K. Arya, R. Babbush, D. Bacon, J. C. Bardin, S. Boixo, D. Buell, B. Burkett, Yu Chen, R. Collins, E. Farhi, A. Fowler, C. Gidney, M. Giustina, R. Graff, M. Harrigan, T. Huang, S. V. Isakov, E. Jeffrey, Z. Jiang, D. Kafri, K. Kechedzhi, P. Klimov, A. Korotkov, F. Kostritsa, D. Landhuis, E. Lucero, J. McClean, M. McEwen, X. Mi, M. Mohseni, J. Y. Mutus, O. Naaman, M. Neeley, M. Niu, A. Petukhov, C. Quintana, N. Rubin, D. Sank, V. Smelyanskiy, A. Vainsencher, T. C. White, Z. Yao, P. Yeh, A. Zalcman, H. Neven, and J. M. Martinis. Demonstrating a Continuous Set of Two-Qubit Gates for Near-Term Quantum Algorithms. *Phys. Rev. Lett.*, 125:120504, Sep 2020.
- [33] Barbara Kraus and Juan I Cirac. Optimal creation of entanglement using a two-qubit gate. *Physical Review A*, 63(6):062309, 2001.
- [34] Navin Khaneja, Roger Brockett, and Steffen J Glaser. Time optimal control in spin systems. *Physical Review A*, 63(3):032308, 2001.
- [35] Marc Grau Davis, Ethan Smith, Ana Tudor, Koushik Sen, Irfan Siddiqi, and Costin Iancu. Heuristics for quantum compiling with a continuous gate set. *arXiv preprint arXiv:1912.02727*, 2019.
- [36] Lingling Lao, Prakash Murali, Margaret Martonosi, and Dan Browne. Designing calibration and expressivity-efficient instruction sets for quantum computing. In *ACM/IEEE 48th Annual International Symposium on Computer Architecture (ISCA)*, pages 846–859, 2021.
- [37] Mohammad Javad Dousti, Alireza Shafaei, and Massoud Pedram. Squash: a scalable quantum mapper considering ancilla sharing. In *Proceedings of the 24th edition of the great lakes symposium on VLSI*, pages 117–122, 2014.
- [38] Tayebbeh Bahreini and Naser Mohammadzadeh. An minlp model for scheduling and placement of quantum circuits with a heuristic solution approach. *ACM Journal on Emerging Technologies in Computing Systems (JETC)*, 12(3):1–20, 2015.
- [39] Lingling Lao, Bas van Wee, Imran Ashraf, J van Someren, Nader Khammassi, Koen Bertels, and Carmen G Almudever. Mapping of lattice surgery-based quantum circuits on surface code architectures. *Quantum Science and Technology*, 4(1):015005, 2018.
- [40] Sartaj Sahni and Teofilo Gonzalez. P-complete approximation problems. *J. ACM*, 23(3):555–565, July 1976.
- [41] Fred Glover. Tabu search—part I. *ORSA Journal on computing*, 1(3):190–206, 1989.
- [42] Fred Glover. Tabu search—part II. *ORSA Journal on computing*, 2(1):4–32, 1990.
- [43] Rainer E Burkard and Franz Rendl. A thermodynamically motivated simulation procedure for combinatorial optimization problems. *European Journal of Operational Research*, 17(2):169–174, 1984.
- [44] Yong Li, Panos M Pardalos, and Mauricio GC Resende. A greedy randomized adaptive search procedure for the quadratic assignment problem. *Quadratic assignment and related problems*, 16:237–261, 1993.
- [45] Swamit S Tannu and Moinuddin K Qureshi. Not All Qubits Are Created Equal: A Case for Variability-Aware Policies for NISQ-Era Quantum Computers. In *Proceedings of the Twenty-Fourth International Conference on Architectural Support for Programming Languages and Operating Systems*, pages 987–999. ACM, 2019.
- [46] Yongshan Ding, Xin-Chuan Wu, Adam Holmes, Ash Wiseth, Diana Franklin, Margaret Martonosi, and Frederic T Chong. SQUARE: strategic quantum ancilla reuse for modular quantum programs via cost-effective uncomputation. In *2020 ACM/IEEE 47th Annual International Symposium on Computer Architecture (ISCA)*, pages 570–583. IEEE, 2020.
- [47] Tommy R Jensen and Bjarne Toft. *Graph coloring problems*, volume 39. John Wiley & Sons, 2011.
- [48] Francisco Barahona. On the computational complexity of ising spin glass models. *Journal of Physics A: Mathematical and General*, 15(10):3241, 1982.
- [49] Lars Onsager. Crystal statistics. i. a two-dimensional model with an order-disorder transition. *Physical Review*, 65(3-4):117, 1944.
- [50] Nathan Lacroix, Christoph Hellings, Christian Kraglund Andersen, Agustin Di Paolo, Ants Remm, Stefania Lazar, Sebastian Krinner, Graham J. Norris, Mihai Gabureac, Johannes Heinsoo, Alexandre Blais, Christopher Eichler, and Andreas Wallraff. Improving the performance of deep quantum optimization algorithms with continuous gate sets. *PRX Quantum*, 1(2):110304, 2020.
- [51] Matthew P Harrigan, Kevin J Sung, Matthew Neeley, Kevin J Satzinger, Frank Arute, Kunal Arya, Juan Atalaya, Joseph C Bardin, Rami Barends, Sergio Boixo, Michael Broughton, Bob B Buckley, David A Buell, Brian Burkett, Nicholas Bushnell, Yu Chen, Zijun Chen, Ben Chiaro, Roberto Collins, William Courtney, Sean Demura, Andrew Dunswoth, Daniel Eppens, Austin Fowler, Brooks Foxen, Craig Gidney, Marissa Giustina, Rob Graff, Steve Habegger, Alan Ho, Sabrina Hong, Trent Huang, L B Ioffe, Sergei V Isakov, Evan Jeffrey, Zhang Jiang, Cody Jones, Dvir Kafri, Kostyantyn Kechedzhi, Julian Kelly, Seon Kim, Paul V Klimov, Alexander N Korotkov, Fedor Kostritsa, David Landhuis, Pavel Laptev, Mike Lindmark, Martin Leib, Orion Martin, John M Martinis, Jarrod R McClean, Matt McEwen, Anthony Megrant, Xiao Mi, Masoud Mohseni, Wojciech Mruczkiewicz,

- Josh Mutus, Ofer Naaman, Charles Neill, Florian Neukart, Murphy Yuezhen Niu, Thomas E O’Brien, Bryan O’Gorman, Eric Ostby, Andre Petukhov, Harald Putterman, Chris Quintana, Pedram Roushan, Nicholas C Rubin, Daniel Sank, Andrea Skolik, Vadim Smelyanskiy, Doug Strain, Michael Streif, Marco Szalay, Amit Vainsencher, Theodore White, Z Jamie Yao, Ping Yeh, Adam Zalcman, Leo Zhou, Hartmut Neven, Dave Bacon, Erik Lucero, Edward Farhi, and Ryan Babbush. Quantum approximate optimization of non-planar graph problems on a planar superconducting processor. *Nature physics*, 17(3):332–336, February 2021.
- [52] Quantum AI team and collaborators. ReCirq, October 2020.
- [53] Cirq Developers. Cirq, May 2021. See full list of authors on Github: <https://github.com/quantumlib/Cirq/graphs/contributors>.
- [54] Rainer E Burkard, Eranda Cela, Panos M Pardalos, and Leonidas S Pitsoulis. The quadratic assignment problem. In *Handbook of combinatorial optimization*, pages 1713–1809. Springer, 1998.
- [55] Chi-Fang Chen, Hsin-Yuan Huang, Richard Kueng, and Joel A Tropp. Quantum simulation via randomized product formulas: Low gate complexity with accuracy guarantees. *arXiv preprint arXiv:2008.11751*, 2020.
- [56] Yingkai Ouyang, David R White, and Earl T Campbell. Compilation by stochastic Hamiltonian sparsification. *Quantum*, 4:235, 2020.
- [57] Paul K Faehrmann, Mark Steudtner, Richard Kueng, Maria Kieferova, and Jens Eisert. Randomizing multi-product formulas for improved Hamiltonian simulation. *arXiv preprint arXiv:2101.07808*, 2021.
- [58] Ewout van den Berg and Kristan Temme. Circuit optimization of Hamiltonian simulation by simultaneous diagonalization of Pauli clusters. *Quantum*, 4:322, 2020.
- [59] Alexander Cowtan, Will Simmons, and Ross Duncan. A generic compilation strategy for the unitary coupled cluster ansatz. *arXiv preprint arXiv:2007.10515*, 2020.
- [60] Alexander Cowtan, Silas Dilkes, Ross Duncan, Will Simmons, and Seyon Sivarajah. Phase gadget synthesis for shallow circuits. *arXiv preprint arXiv:1906.01734*, 2019.
- [61] Arianne Meijer-van de Griend and Ross Duncan. Architecture-aware synthesis of phase polynomials for NISQ devices. *arXiv preprint arXiv:2004.06052*, 2020.
- [62] Prakash Murali, David C McKay, Margaret Martonosi, and Ali Javadi-Abhari. Software Mitigation of Crosstalk on Noisy Intermediate-Scale Quantum Computers. In *Proceedings of the Twenty-Fifth International Conference on Architectural Support for Programming Languages and Operating Systems*, pages 1001–1016, 2020.
- [63] Pierre-Luc Dallaire-Demers and Frank K Wilhelm. Quantum gates and architecture for the quantum simulation of the Fermi-Hubbard model. *Physical Review A*, 94(6):062304, 2016.
- [64] Gushu Li, Yunong Shi, and Ali Javadi-Abhari. Software-hardware co-optimization for computational chemistry on superconducting quantum processors. *arXiv preprint arXiv:2105.07127*, 2021.
- [65] Pranav Gokhale, Yongshan Ding, Thomas Propson, Christopher Winkler, Nelson Leung, Yunong Shi, David I Schuster, Henry Hoffmann, and Frederic T Chong. Partial compilation of variational algorithms for noisy intermediate-scale quantum machines. In *Proceedings of the 52nd Annual IEEE/ACM International Symposium on Microarchitecture*, pages 266–278, 2019.
- [66] Kristan Temme, Sergey Bravyi, and Jay M. Gambetta. Error mitigation for short-depth quantum circuits. *Phys. Rev. Lett.*, 119:180509, Nov 2017.
- [67] Ying Li and Simon C. Benjamin. Efficient variational quantum simulator incorporating active error minimization. *Phys. Rev. X*, 7:021050, Jun 2017.
- [68] Sergey Bravyi, Sarah Sheldon, Abhinav Kandala, David C. McKay, and Jay M. Gambetta. Mitigating measurement errors in multiqubit experiments. *Phys. Rev. A*, 103:042605, Apr 2021.
- [69] Swamit S Tannu and Moinuddin K Qureshi. Mitigating measurement errors in quantum computers by exploiting state-dependent bias. In *Proceedings of the 52nd Annual IEEE/ACM International Symposium on Microarchitecture*, pages 279–290, 2019.

A. Appendix

In this appendix, we present additional results of comparing 2QAN’s compilation performance on the IBM Montreal, Google Sycamore, and Rigetti Aspen devices. In addition to the hardware two-qubit gates (SYC and iSWAP) in Figure 1,

Sycamore and Aspen also implement CZ gates as native gates. In this comparison, we use the recommended optimization passes for the CNOT/CZ gates in Qiskit and $t|ket\rangle$, that is, Qiskit with optimization level 3 and $t|ket\rangle$ with the ‘FullPass’ (FullPeepholeOptimise, followed by the default qubit mapping pass, SynthesiseIBM). Similarly to results in Section 5, 2QAN exploits the term permutation flexibility in Hamiltonian simulation and has the *least compilation overhead* (the number of inserted SWAPs, the CNOT gate count, and the circuit depth) compared to Qiskit and $t|ket\rangle$ across all benchmarks and quantum computers.

Figure 11 shows the compilation results of 3-layer QAOA on the Montreal device. Since QAOA has periodic circuit structures, the 3-layer QAOA circuits have approximately 3x compilation overhead compared to 1-layer QAOA circuits in Figure 9. Figure 12 and Table 3 show the compilation results on the Sycamore architecture with CZ as the hardware two-qubit gate. 2QAN almost has *no CZ overhead* compared to ‘NoMap’ for the Heisenberg model. This is because most of the SWAPs can be combined with circuit gates (Figure 12a) and such an unified gate can be decomposed into the same number (3) of CZs as a circuit gate $\exp(i(\alpha XX + \beta YY + \gamma ZZ))$. In contrast, $t|ket\rangle$ and Qiskit lead to on average 55.6% and 107% CZ overhead, respectively. Similarly, 2QAN only has on average 8.7% CZ overhead for the Ising model (the circuit unitary $\exp(i\theta ZZ)$ requires 2 CZs). The maximum depth reduction over three benchmarks is 10.3x relative to $t|ket\rangle$ and 13.7x compared to Qiskit. Figure 13 and Table 4 show the results of compilation on the Aspen architecture. 2QAN inserts the same number of SWAPs as $t|ket\rangle$ for both the Heisenberg model and the Ising model. More than 60% of these SWAPs can be combined with circuit gates, which will help reduce hardware gate count. For example, 2QAN reduces CZ overhead of the Heisenberg model by on average 2.8x (up to 3.0x) compared to $t|ket\rangle$ and 7.2x (up to 9.3x) with respect to Qiskit. The average depth reduction over three benchmarks is 1.6x and 2.9x compared to $t|ket\rangle$ and Qiskit, respectively.

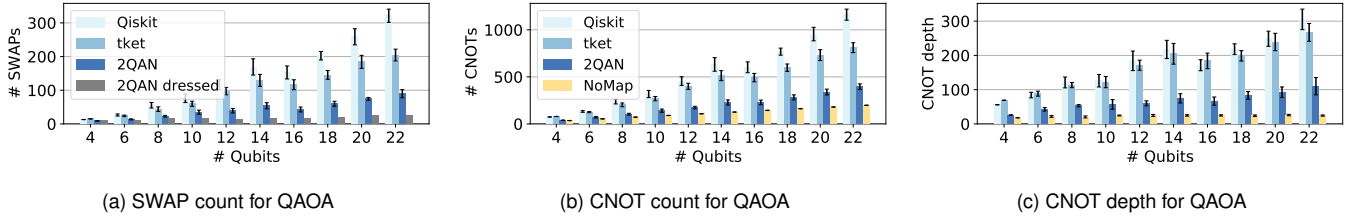


Figure 11: Compilation results of 3-layer QAOA on the IBMQ Montreal device. Each QAOA problem size is averaged over 10 different instances (error bars show the standard deviation) and operator parameters of QAOA circuits were chosen at their theoretically optimal values. ‘2QAN dressed’ shows the number of SWAPs that were merged with circuit gates by 2QAN, which helps to reduce hardware gate count. ‘NoMap’ represents the compilation results when assuming all-to-all qubit connectivity. The overhead of 3-layer QAOA circuits is approximately 3 times of the overhead of 1-layer QAOA circuits. The 2QAN compiler has least compilation overhead compared to Qiskit and tket).

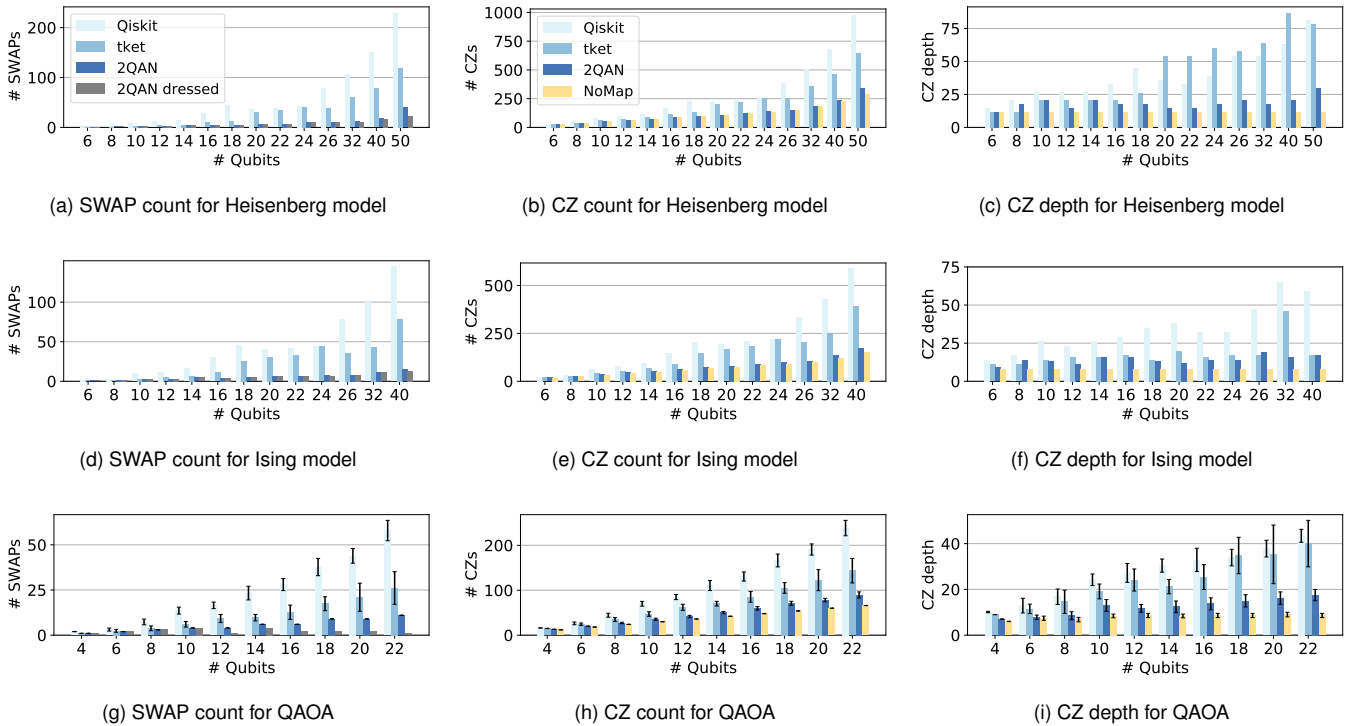


Figure 12: Compilation results of the one-layer NNN Heisenberg model, NNN Ising model, and QAOA on the Google Sycamore architecture with CZ as hardware gate. The 2QAN compiler has least compilation overhead compared to Qiskit and tket).

	tket						Qiskit					
	SWAPs		CZs		Depth		SWAPs		CZs		Depth	
	avg	max	avg	max	avg	max	avg	max	avg	max	avg	max
Heisenberg	3.3x	5x	–	–	2.2x	4.1x	5.1x	9x	–	–	2.1x	3x
Ising	2.6x	5x	8.7x	15.6x	1.3x	2.9x	5.2x	8.9x	16.4x	29.6x	2.4x	4.1x
QAOA	1.8x	2.4x	3.4x	4.8x	4.3x	10.3x	3.6x	5.3x	6.7x	9x	5.5x	13.7x

Table 3: The average (avg) and maximum (max) compilation overhead reduction when comparing 2QAN with tket and Qiskit on the Sycamore architecture with CZ as hardware gate. For the cases with no values ‘–’, 2QAN has negligible CZ overhead.

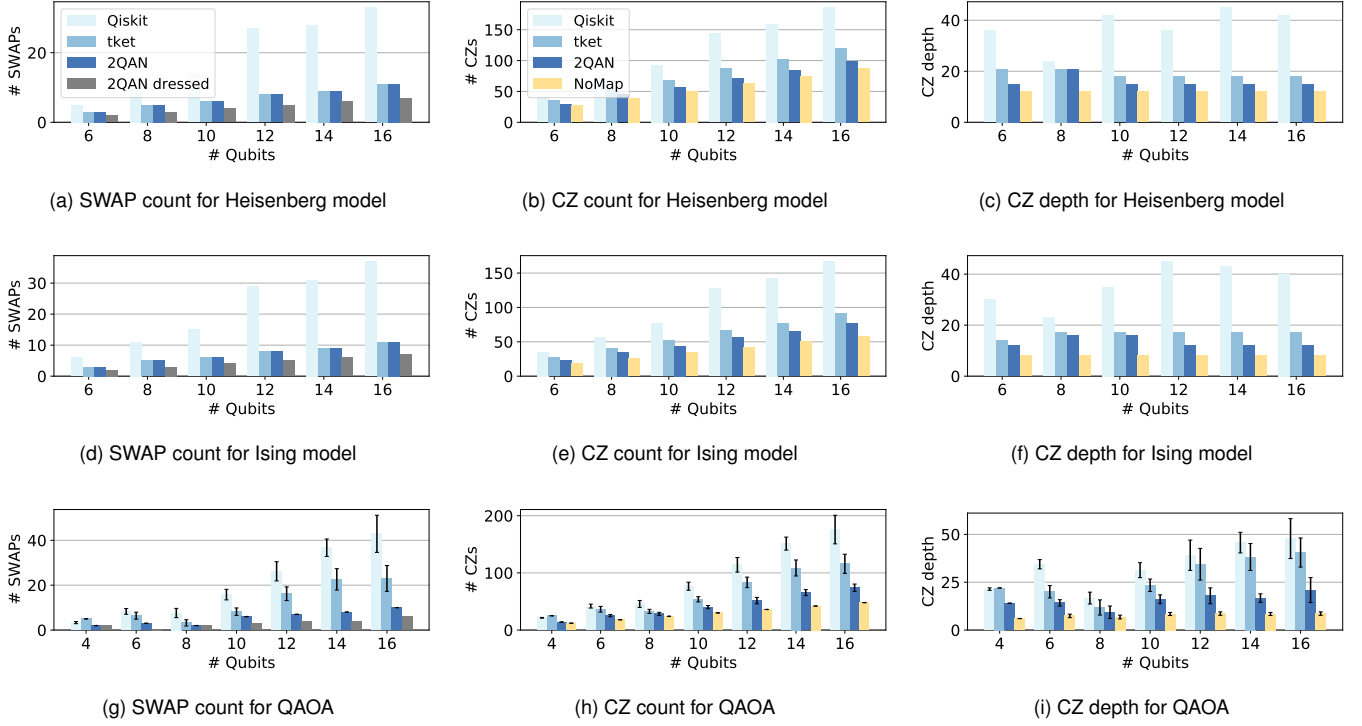


Figure 13: Compilation results of the one-layer NNN Heisenberg model, NNN Ising model, and QAOA on the Rigetti Aspen architecture with CZ as hardware gate. The 2QAN compiler has least compilation overhead compared to Qiskit and t|ket.

	t ket)						Qiskit					
	SWAPs		CZs		Depth		SWAPs		CZs		Depth	
	avg	max	avg	max	avg	max	avg	max	avg	max	avg	max
Heisenberg	1x	1x	2.8x	3x	1.2x	1.4x	2.7x	3.5x	7.2x	9.3x	2.4x	3x
Ising	1x	1x	1.7x	1.8x	1.2x	1.4x	2.7x	3.5x	4.9x	6.2x	2.8x	3.7x
QAOA	2.1x	2.8x	3.1x	6.5x	2.4x	3.6x	3.3x	4.6x	4.6x	5x	3.4x	4.6x

Table 4: The average (avg) and maximum (max) compilation overhead reduction when comparing 2QAN with t|ket) and Qiskit on the Aspen architecture with CZ as hardware gate.